AJNR

Half-Fourier MR imaging of CNS disease.

V M Runge and M L Wood

AJNR Am J Neuroradiol 1990, 11 (1) 77-82
http://www.ajnr.org/content/11/1/77

Half-Fourier MR Imaging of CNS Disease

Val M. Runge[1]
Michael L. Wood[2]

Three MR imaging techniques were compared in 37 CNS examinations. In each case, postprocessing of a single data set in three different ways was used for comparison. Eleven of the 37 patients had a clinical diagnosis of multiple sclerosis. The primary purpose of this investigation was to evaluate the quality of the half-Fourier imaging technique. With half-Fourier imaging, scan time can be reduced by approximately half without compromising spatial resolution. In T2-weighted examinations at 1.0 T (with present instrumentation), application of the half-Fourier technique leads to a decrease in lesion detectability in patients with multiple sclerosis: this is because there is a reduction in the signal difference-to-noise ratio of 32 ± 11%.

For T2-weighted screening of the CNS on high-field MR systems, with the exception of multiple sclerosis, half-Fourier imaging may offer a suitable compromise by decreasing scan time while preserving spatial resolution. Application of the half-Fourier method to T1-weighted techniques also results in diagnostic-quality images.

***AJNR* 11:77–82, January/February 1990**

With the advent of half-Fourier MR imaging, the possibility of further decreases in imaging time emerges [1–6]. Normally, the phase-encoding gradient is stepped through a range of dual polarity. The larger the maximum amplitude, the greater the spatial resolution in the resulting image. There is conjugate symmetry [6] between the data for the phase-encoding steps of one polarity and that of the other polarity; therefore, it is not strictly necessary to acquire the data for these other phase-encoding steps. To the extent that the data are free of imperfections, images can be formed from the phase-encoding steps of a single polarity. This constitutes the basis for half-Fourier imaging. Thus, scan time can be cut approximately in half without a loss in spatial resolution.

To evaluate this new technique, 37 patients with a spectrum of CNS pathology were scanned. Eleven patients with multiple sclerosis were included to judge the effectiveness of half-Fourier imaging in detecting small, relatively low-contrast lesions [7]. The results of half-Fourier imaging were compared with those from conventional techniques that used both 256 and 128 phase-encoding steps.

Received May 26, 1988; revision requested July 29, 1988; revision received July 17, 1989; accepted August 21, 1989.

[1] Department of Radiology, New England Medical Center Hospitals, 750 Washington St., Box 864, Boston, MA 02111. Address reprint requests to V. M. Runge.

[2] Department of Radiation Oncology and Medical Physics, New England Medical Center Hospitals, Boston, MA 02111.

0195–6108/90/1101–077

Materials and Methods

The MR imaging data from 37 patient examinations were saved and later reconstructed into images. All examinations were conducted at 1.0 T on a Siemens Magnetom (Siemens Medical Systems; Iselin, NJ). Both T1-weighted, 800/17/2 (TR/TE/excitations), and T2-weighted, 3000/28,70/1, images were employed. The slice thickness was 10 mm, with no gap (permitted by use of a computer-optimized slice profile) and a 25-cm field of view. Three reconstruction techniques were used in each case. All began with a global phase correction, which helped symmetrize the data and shifted the desirable image intensity into the real component of the complex MR images. The normal technique used all 256 phase-encoding steps (−127 to 128). The second technique used only one half the data, specifically the steps

−63 to 64, inclusively. This produced a rectangular pixel matrix with an intrinsic resolution of 256 × 128 steps. Third was the half-Fourier imaging technique developed by Margosian and Schmitt [5]. Here, phase-encoding steps −8 to 128 were used, which accounted for 53% of the data. A Hamming filter was applied to reduce truncation artifacts. Had the data been reconstructed in line, image reconstruction time would have been longer for half-Fourier imaging than for the conventional technique, which used 256 phase-encoding steps with present instrumentation (11 vs 5 sec/slice).

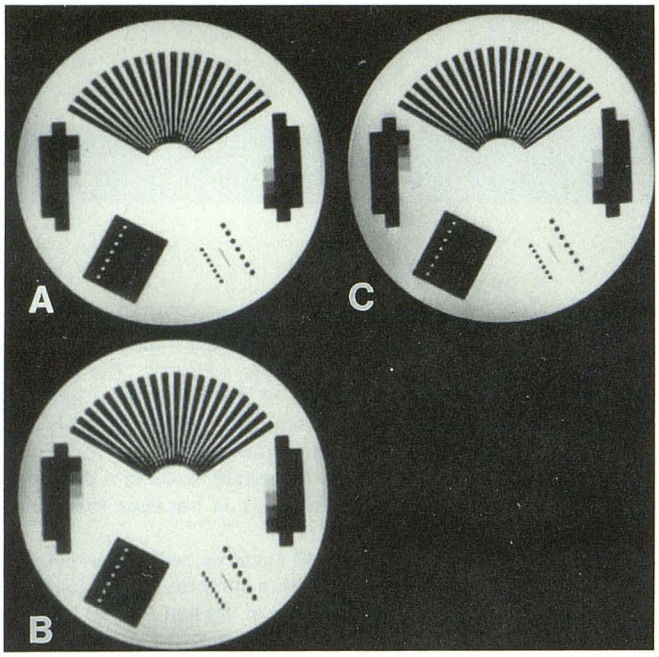

Fig. 1.—Compromises in signal/noise ratio and resolution with half-Fourier imaging and rectangular pixels. The images are of a phantom, and were reconstructed in three different ways from the same data: *A* is a reference image acquired with 256 phase-encoding steps; *B* is a rectangular pixel image; *C* is a half-Fourier image. The signal/noise ratio in *C* was 27% less that of *A*. The point at which the bars are blurred is the same for *A* and *C*, indicating that resolution was the same. Compare this with the lower resolution of the rectangular pixel image.

The signal/noise ratio (SNR) and signal difference/noise ratio (SD/N) were defined as follows:

$$\text{SNR} = (\text{mean image intensity})/(\text{standard deviation of noise})$$

$$\text{SD/N} = (\text{SNR of one tissue} - \text{SNR of other tissue})$$

Measurements were performed with the use of computer-drawn regions of interest. The SD/N between gray and white matter was compared for the three techniques. These results were expressed as a percent change from the 256 × 256 acquisition, which was employed as the reference standard. In the multiple sclerosis patients, lesion detectability was judged by an independent reading of the films (17 different levels in 11 patients) by four radiologists with MR experience. The films were presented in random order and in a blinded fashion for interpretation. The readers were instructed to count the number of plaques visible on each examination, using their own clinical experience to define what constitutes a lesion. The SD/N between multiple sclerosis plaques and surrounding presumed normal white matter was also quantified.

In addition to the 11 cases of multiple sclerosis, diagnoses included (with number of patients in parentheses): neoplasia (5), ischemic/gliotic changes (2), infarction (2), posttraumatic encephalomalacia (1), atrophy (1), anoxic injury (1), eosinophilic granuloma (1), neurofibromatosis (1), arteriovenous malformation (1), arachnoid cyst (1), Dandy Walker malformation (1), Chiari I malformation (1), and normal (8).

These latter studies were examined qualitatively with respect to diagnostic utility. Quantitative examination was, however, confined to the multiple sclerosis group because of its more homogeneous character and amenability to statistical analysis (detection of multiple small punctate lesions).

Results

Phantom studies demonstrated the preservation of spatial resolution with the half-Fourier imaging technique (Fig. 1). However, the loss of redundancy in data led to noisier images.

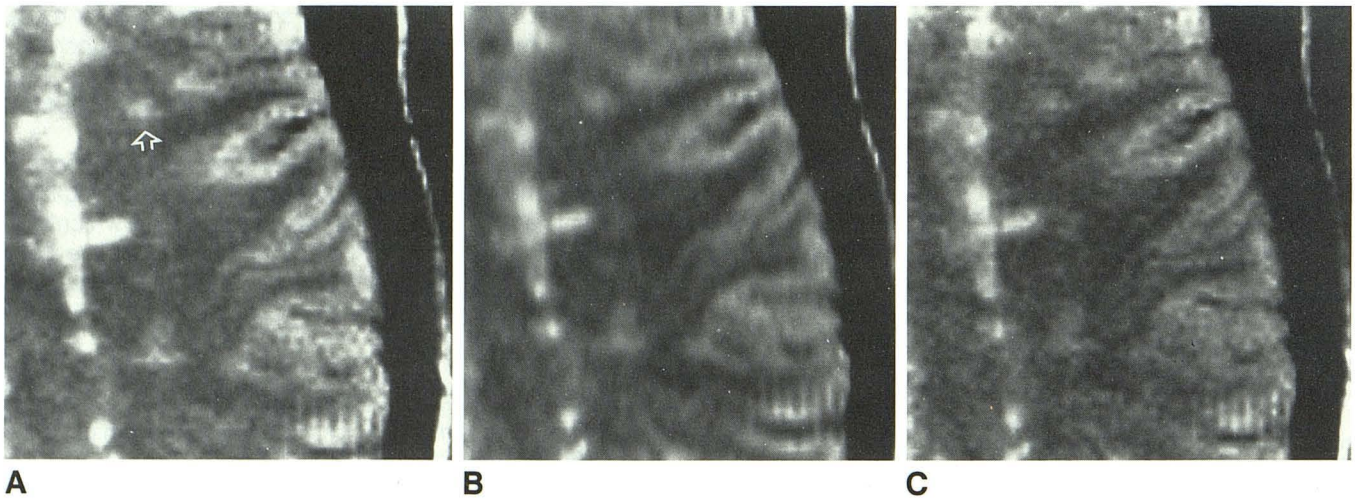

Fig. 2.—*A–C*, All images acquired with TR = 3000, TE = 28. *A* is a reference image with 256 × 256 matrix and one acquisition; *B* is a rectangular pixel image with 256 × 128 matrix and one acquisition; *C* is a half-Fourier image. Had the entire data set not been collected prospectively, the scan times for the three techniques would have been 12.8 min (*A*), 6.4 min (*B*), and 6.8 min (*C*). The diagnosis was multiple sclerosis. Use of rectangular pixels improves the ability to visualize small white-matter lesions despite the poor resolution when compared with a 256 × 256 matrix. With the half-Fourier technique, some small lesions become more difficult to identify (*arrow* in *A*) because of the limited signal difference/noise ratio. To facilitate this comparison of techniques, each image has been magnified and only a portion of the left cerebral hemisphere displayed.

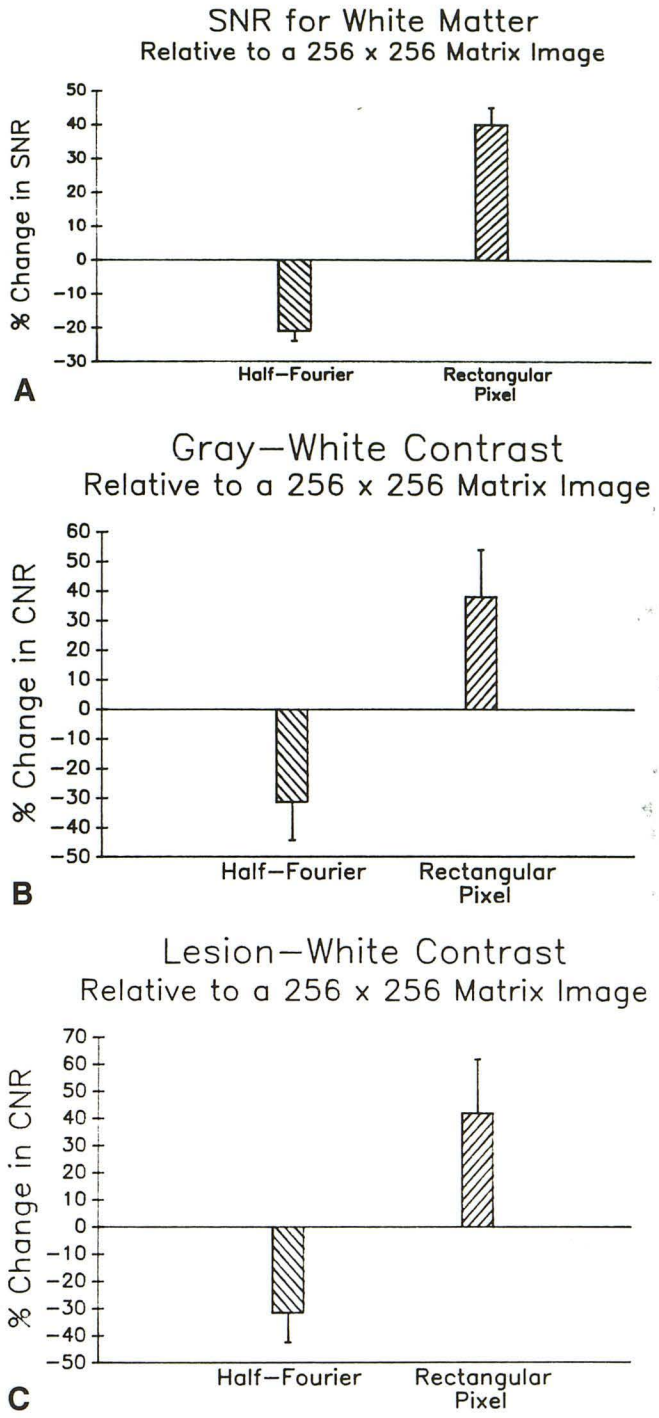

Fig. 3.—Comparison of half-Fourier imaging and rectangular pixels by the use of region of interest analysis. The percent change with respect to a 256 × 256 matrix is graphed. *A* = signal/noise ratio (SNR) from white matter, *n* = 19; *B* = percent change in contrast/noise ratio for gray vs white matter, *n* = 19; *C* = percent change in contrast/noise ratio for multiple sclerosis plaques vs surrounding normal white matter, *n* = 10.

Clinical review of the 37 patient examinations revealed the preservation of detail for high-contrast structures, such as blood vessels, with the half-Fourier technique. However, a loss in visualization of low-contrast lesions was noted. Thus, in Figure 2, more multiple sclerosis plaques can be identified in the true 256 × 256 acquisition (Fig. 2A) than in the half-Fourier acquisition (Fig. 2C). The lesions were most apparent on the rectangular pixel image (Fig. 2B). However, the 256 × 256 matrix image was preferred by all readers because of its high intrinsic spatial resolution.

Analysis of the 3000/28 images from 19 patients revealed a loss of 21 ± 3% ($p < .0001$) in the SNR of white matter for the half-Fourier technique compared with a standard acquisition with 256 phase-encoding steps (Fig. 3A). Use of a rectangular pixel matter (256 × 128) improved the SNR by 40 ± 5% ($p < .0001$).

The loss in SNR with half-Fourier imaging leads to a loss in gray-white SD/N (Fig. 3B). Thus, lesion-white matter SD/N would also be anticipated to decrease with half-Fourier imaging, agreeing with experimental results obtained from a multiple sclerosis patient population (Fig. 3C, $n = 10$).

The SD/N between gray and white matter decreased by 31 ± 13% ($n = 19$, $p < .0001$) with the half-Fourier technique, but increased 38 ± 16% ($p < .0001$) with rectangular pixels. The SD/N between multiple sclerosis lesions and normal surrounding white matter decreased by 32 ± 11% ($n = 10$, $p < .0001$) with the half-Fourier technique and increased by 42 ± 20% ($p < .0001$) with rectangular pixels.

A blinded evaluation of the 3000/28 images by four radiologists revealed a statistically significant ($p < .001$) decrease in lesion detection in multiple sclerosis patients with half-Fourier imaging (Fig. 4). The rectangular pixel matrix (central 128 phase-encoding steps) proved superior ($p < .025$) to both half-Fourier imaging and the 256 × 256 matrix for lesion detection in multiple sclerosis. On a later, more T2-weighted, echo (Fig. 5), the rectangular pixel matrix remained superior for demonstration of multiple sclerosis plaques. Once again, the SD/N proved to be the limiting factor.

On T1-weighted images (Fig. 6), use of the rectangular pixel matrix led to an unacceptable blurring of fine detail. This finding was noted consistently within the group of 37 examinations. For illustration, compare the sharp delineation of the cortical sulci (*arrow* in Fig. 6C) seen by the half-Fourier technique to that in *B*, the rectangular pixel matrix. The

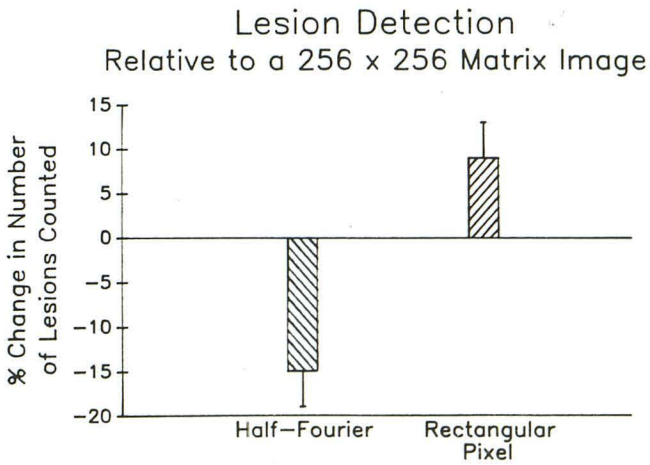

Fig. 4.—Blinded reader evaluation of the 11 multiple sclerosis examinations. Percent increase or decrease in the number of lesions counted compared with a standard 256 × 256 acquisition.

anatomic detail of high-contrast structures was preserved with half-Fourier imaging.

In comparing conventional and half-Fourier images, a slight difference in vessel and CSF pulsation artifact was noted. This was not consistently more evident with one technique. For example, in some instances there was a greater loss in CSF signal intensity in the prepontine space with half-Fourier imaging (with T2-weighted images), while in other cases this loss was greater with the conventional 256 × 256 matrix.

Discussion

With half-Fourier imaging [5, 6], acquisition time is approximately halved with preservation of spatial resolution. Thus, fine detail for high-contrast structures such as blood vessels is retained. However, the decrease in SNR and thus SD/N with half-Fourier imaging leads to loss in low-contrast lesion visualization. This was confirmed statistically in a multiple sclerosis patient population. These conclusions were made from images acquired with a technique that used a computer-optimized slice profile for improved contrast. According to basic principles, a 27% loss in SNR (or SD/N) is anticipated with a twofold reduction in acquisition time. Experimental results, expressed in Figure 3 as a percent change from the 256 × 256 acquisition, confirm this prediction.

The SD/N with the rectangular pixel was greater than that with either a 256 × 256 matrix or half-Fourier technique, as anticipated. Blinded reader evaluation of the 11 multiple sclerosis cases demonstrated that rectangular pixels were superior for lesion detection, despite the fact that resolution along

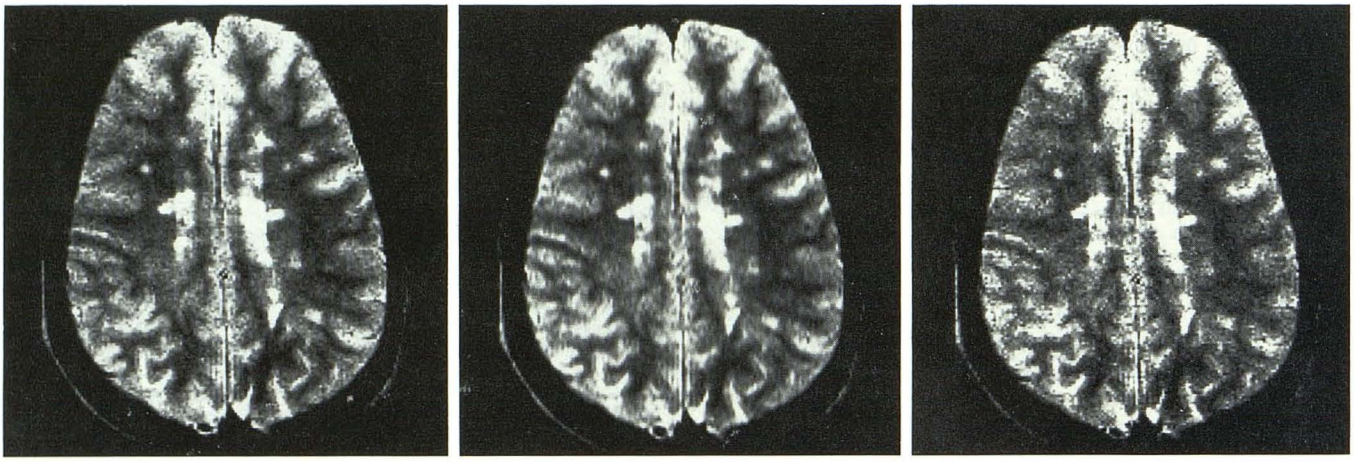

Fig. 5.—*A–C*, All images acquired with TR = 3000, TE = 70. *A* = 256 × 256 matrix; *B* = rectangular pixel; *C* = half-Fourier image. The diagnosis was multiple sclerosis. On the more T2-weighted examination, the rectangular pixel matrix again proved superior for identification of small white-matter plaques.

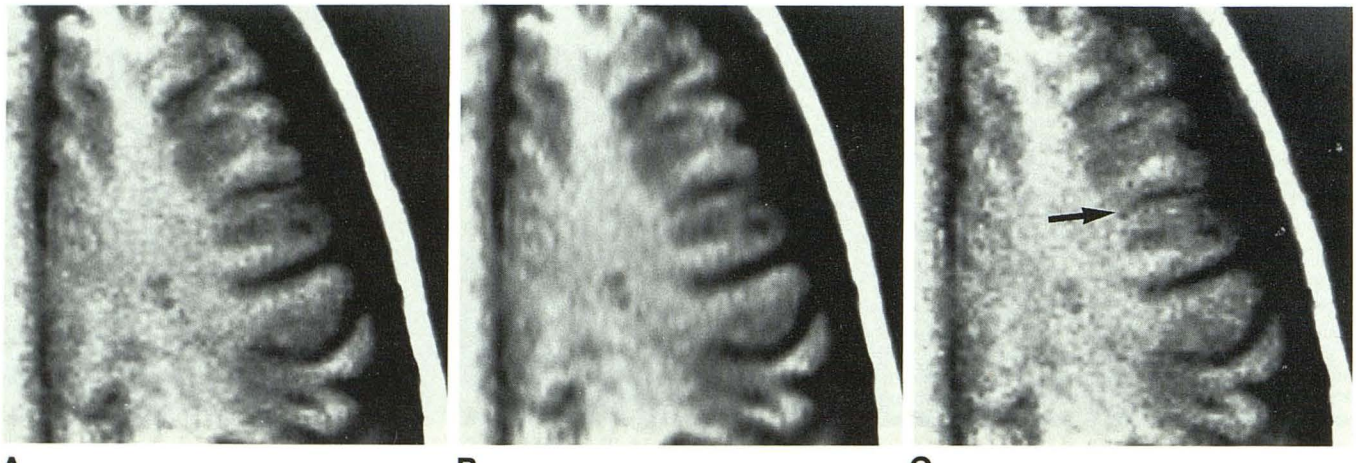

Fig. 6.—*A–C*, All images acquired with TR = 600, TE = 17. *A* = 256 × 256 matrix; *B* = rectangular pixel; *C* = half-Fourier image. The diagnosis was multiple sclerosis. On T1-weighted images, the half-Fourier technique substantially decreased scan time while preserving spatial resolution of high-contrast structures (*arrow* in *C*). Unfortunately, the signal/noise ratio is markedly reduced, leading to the grainy appearance of the half-Fourier image. All three images are magnified to the same degree, with only a portion of the left cerebral hemisphere displayed, in order to facilitate comparison.

the phase-encoding direction was sacrificed. Thus, the SD/N proved to be the limiting factor for lesion detection.

One potential pitfall in this study is the lack of a reference standard for lesion count. In this instance, only gross pathology could serve in such a role, a correlation not possible because of the chronic nature of disease progression in multiple sclerosis. Each reader, however, consistently identified a larger number of lesions on the rectangular pixel images. False-positive lesion identification was not thought to be a potential factor by virtue of reader experience, the presentation of films in a blinded and randomized fashion, and constancy of imaging parameters between studies with the sole exception of matrix size.

Future improvements in SNR resulting from the use of higher field systems, better RF coils (quadrature detection), or lower bandwidth pulse sequences could impact the use of half-Fourier imaging. In this instance, SNR might not be the limiting factor for detection of multiple sclerosis plaques, leading to adoption of half-Fourier imaging as the technique of choice because of its high spatial resolution and short scan time. However, one caveat remains. The present research was performed with 1-cm-thick sections. In this setting, the potential for missing lesions because of volume averaging arises. If thinner sections are employed, SNR decreases, potentially limiting the application of half-Fourier imaging.

In areas of motion, such as CSF pulsation, a further difference may arise between half-Fourier imaging and conventional methods. Sampling with both positive and negative phase-encoding gradient values can lead to some diminution of motion artifacts in analogy with data averaging. In clinical application, this effect proved to be minimal. However, CSF pulsation and blood flow can potentially be the source of significant artifacts on half-Fourier images of the brain. This necessitates routine use of motion-compensation techniques such as gradient-moment nulling and/or ECG gating to obtain diagnostic-quality scans with half-Fourier imaging.

In the examination of neoplastic disease, the criteria for lesion detection change. By the time of clinical presentation, neoplastic lesions (including the surrounding cerebral edema that they elicit) are often large and demonstrate high contrast on T2-weighted images when compared with surrounding normal brain. In this circumstance, as demonstrated within the clinical population examined (Fig. 7), half-Fourier imaging may play an important role by reducing scan time yet preserving spatial resolution.

Application of half-Fourier imaging to a high SNR T1-weighted technique resulted in clinically acceptable image quality. T1-weighted spin-echo scans are most often employed in clinical practice for depiction of anatomic or structural detail. Lesion detection on these scans in the brain is typically not based on a difference in tissue contrast (with the exception of high-signal-intensity abnormalities, such as that produced by hemorrhage, fat, or Gd-DTPA enhancement). Thus, the half-Fourier technique can be used to advantage, with scan time halved and spatial resolution preserved. The T1-weighted images in this study were performed with two excitations and the use of a linear polarized receiver coil. With quadrature coils and higher field systems, single excitation scans are now routine for brain screening. Our intent was to demonstrate the potential efficacy of half-Fourier imaging under these circumstances. With newer-generation equipment, SNR is less of a limitation, and half-Fourier imaging may be applied to reduce scan time on examinations acquired with a single excitation.

Recent work [8] suggests that half-Fourier imaging with two excitations theoretically should produce images of similar quality when compared with a single excitation 256 × 256 matrix. However, artifacts can arise from various sources, including motion, favoring the use of a standard matrix in this instance. Thus, the application of half-Fourier imaging will most likely be with scans that do not employ data averaging.

As noted earlier, in screening for intracranial neoplastic disease, half-Fourier imaging may offer a suitable compromise. High spatial resolution T2-weighted images can be obtained in 5 min or less. This technique is best suited for the detection of high-contrast lesions. Owing to SNR limitations,

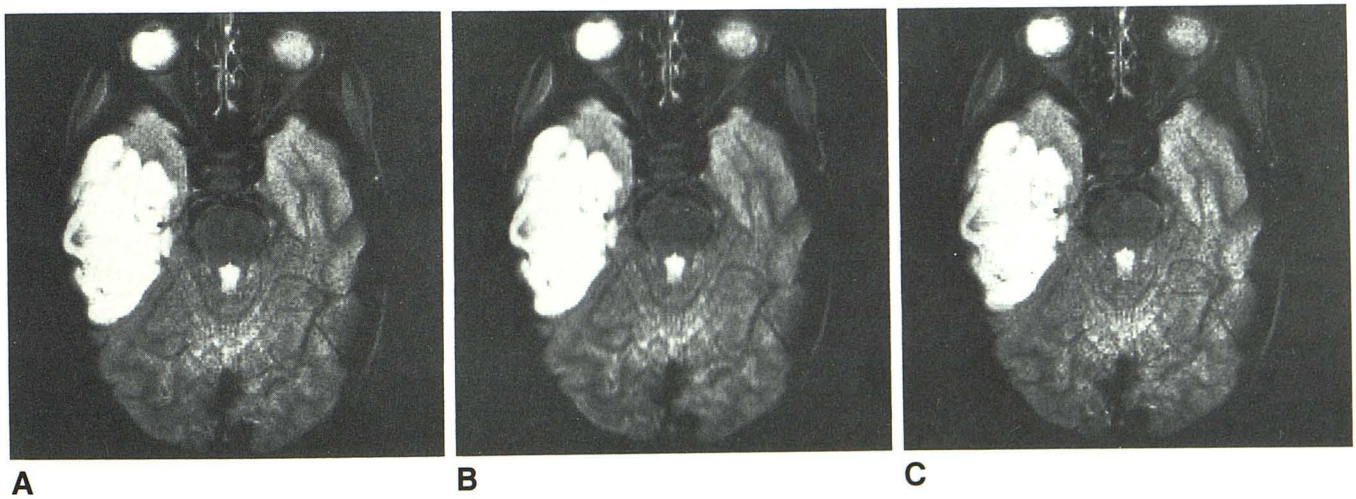

Fig. 7.—*A–C*, All images acquired with TR = 3000, TE = 70. *A* = 256 × 256 matrix; *B* = rectangular pixel; *C* = half-Fourier image. The diagnosis was low-grade astrocytoma. The lesion was well identified by all three techniques.

its application is more likely on high-field-strength systems equipped with quadrature coils. The principles involved in half-Fourier imaging can also be applied to produce images that incorporate larger numbers of views (between 136 and 256). This technique is referred to generically as partial-Fourier imaging [9]. With less missing data, artifacts are reduced; however, the trade-off between SNR and acquisition time remains. In the future, a premium may also be placed on the ability to acquire the entire data for a single slice in less than 10 sec, in order to achieve breath-hold images of the abdomen. It is hoped that the half-Fourier technique can be applied successfully with gradient-echo pulse sequences. It may then also play a major role in rapid single-slice acquisition techniques.

Appendix

The dependence of SNR on basic imaging parameters [10] can be described as follows:

$$SNR = k_1 \frac{(FOV)^2 \, W_{slice} \, (N_{av} \, T_s)^{1/2}}{N_{read} \, (N_{phase})^{1/2}}$$

where FOV = field of view, W_{slice} = slice thickness, N_{av} = number of data measurements averaged (i.e., NEX), T_s = time to measure each NMR signal, N_{read} = number of measurements of each NMR signal, N_{phase} = number of phase-encoding steps of one polarity.

In the comparison discussed, only N_{phase} and N_{av} were allowed to vary. Thus, the equation for SNR can be simplified as follows:

$$SNR = k_2 \frac{(N_{av})^{1/2}}{(N_{phase})^{1/2}}$$

k_1 and k_2 are constants that incorporate other factors not considered in this discussion.

The values of N_{phase} and N_{av} for the three techniques were, respectively

N_{phase}	N_{av}	Technique
128	1	Standard matrix (256 × 256)
64	1	Rectangular pixel matrix
128	0.53	Half-Fourier imaging

N_{av} is 1 for a single acquisition. For partial Fourier imaging, N_{av} is defined as the number of phase-encoding steps (of both polarities) performed divided by the number of phase-encoding steps for the equivalent conventional acquisition. In the case considered for half-Fourier imaging,

$$N_{av} = \frac{128 + 8}{256} = 0.53$$

Substituting these numbers into the equation for SNR, the following results are obtained (with the standard matrix assigned a reference value of 1):

SNR	Technique
1	Standard matrix
1.41	Rectangular pixel matrix
0.73	Half-Fourier imaging

Thus, from a theoretical point of view, a rectangular pixel should have approximately 41% greater SNR than the equivalent square standard matrix, with half-Fourier imaging manifesting a loss of approximately 27%.

REFERENCES

1. Young IR. Considerations affecting signal and contrast in NMR imaging. *Br Med Bull* **1984**;40:139–147
2. Kneeland JB, Knowles RJR, Cahill PT. Magnetic resonance imaging systems: optimization in clinical use. *Radiology* **1984**;153:473–478
3. Koehler PR, Daniels DL, Williams AL, Haughton VM. Technical factors in MR image quality. *Neuroradiology* **1986**;28:74–77
4. Kumar A, Welti D, Ernst RR. NMR Fourier zeugmatography. *J Magn Reson* **1975**;18:69–83
5. Margosian P, Schmitt F. Faster MR imaging: imaging with half the data. *Health Care Instrumentation* **1986**;1:195–197
6. Feinberg DA, Hale JD, Watts JC, Kaufman L, Mark A. Halving MR imaging time by conjugation: demonstration at 3.5 kG. *Radiology* **1986**;161:527–531
7. Lukes SA, Crooks LE, Aminoff MJ, et al. Nuclear magnetic resonance imaging in multiple sclerosis. *Ann Neurol* **1983**;13:592–601
8. Wood ML, Runge VM. Motion artifact reduction by averaging in half-Fourier MR imaging. *Radiology* **1988**;169(P)[Suppl]:326
9. MacFall JR, Pelc NJ, Vavrek RM. Correction of spatially dependent phase shifts for partial Fourier imaging. *Magn Reson Imaging* **1988**;6:143–155
10. Wehrli FW. Principles of magnetic resonance. In: Stark DD, Bradley WG, eds. *Magnetic resonance imaging*. St. Louis: Mosby, **1988**